Proc. 3rd Symposium on Biological Effects and Characterization of Ultrasound Sources 1977, P. 182-195

PRELIMINARY REPORT ON MORPHOLOGICAL CHANGES TO MOUSE TESTICULAR TISSUE FROM IN VIVO ULTRASONIC IRRADIATION

W. D. O'Brien, Jr., J. K. Brady, C. N. Graves*, and F. Dunn

Bioacoustics Research Laboratory
University of Illinois
Urbana, Illinois 61801

and

Department of Dairy Science*
University of Illinois
Urbana, Illinois 61801

INTRODUCTION

Use of ultrasonic diagnostic equipment on, or in close proximity to, the male reproductive organs appears to be increasing (Miskin and Bain, 1974; Albright and Harris, 1975). At present, no data exists upon which to base risk assessment for exposure to ultrasound of the testes.

A study has been initiated for the purpose of providing basic information regarding the interaction between ultrasound and mouse testicular tissue. A portion of this work concerning the ultrasonic absorption coefficient of testicular tissue has been reported (Brady et al., 1976). This paper deals with a continuation of that work in which ultrasonically induced morphological changes in the testis are examined.

Testes are the principal male organ which produce spermatozoa. The production of spermatozoa is called spermatogenesis and consists of spermatocytogenesis and spermiogenesis. In the mouse spermatocytogenesis begins with a stem cell or type A spermatogonium which gives rise to a smaller type B spermatogonium through the intermediate spermatogonium. Type B spermatogonium either divide or metamorphose into primary spermatocytes which has two set of chromosomes. The first meiotic division of the primary spermatocyte yields two haploid secondary spermatocytes. The second meiotic division yields four spermatids, each with one set of monovalent chromosomes, which signals the beginning of spermiogenesis. Spermiogenesis, the transformation of a spermatid into a spermatozoon, involves no divisions. At any given cross-sectional segment of the seminiferous tubule type A spermatogonia are initiating the spermatogenesis cycle which will liberate spermatozoa some 34.5 days later. Spermatocytogenesis requires approximately 25 days and spermiogenesis 9.5 days. This cycle is initiated every 8.6 days (Monesi, 1972; Rugh, 1968; Nalbandov, 1976)

MATERIALS AND METHODS

In vivo testicular irradiation of LAF_1/J mice (Jackson Labs, Bar Harbor, Maine) proceeded by anesthetizing the 5-7 month old males with methoxyfluorane (Hall, 1971), shaving the scrotum and surrounding inguinal regions, bathing the shaved region in a mild detergent to assure wetting of the surface by the coupling medium and mounting the animal in a specially designed supporting structure (holder) to insure that the testes were suspended in the scrotum. Observations post irradiation showed that the testes did not retract into the abdominal cavity. The holder was positioned in the Lucite(R) irradiation tank and 37°C degassed mammalian ringers served as the coupling medium

between the 1 MHz ultrasonic source and the scrotum. Acoustic absorbing material lined portions of the tank to minimize reflections.

The reported ultrasonic intensity represents the free field value determined by the Bioacoustics Research Laboratory calibration facility to a precision of ± 2% (Dunn and Fry, 1972).

The spatial peak intensities employed in this study were 0 W/cm^2 (sham), 10 W/cm^2 and 25 W/cm^2, the latter two requiring different transducers with half-power beam widths of 10 mm and 6mm, respectively, as determined by the transient thermoelectric technique (Dunn and Fry, 1972; O'Brien, 1977). All exposure times were for 30 sec and both testes were sequentially exposed by positioning the beam axis in the center of each testis. No attempt was made to shield accoustically the adjacent testis. Ample time (within a couple of minutes) was allowed for testicular tissue to reach thermal equilibrium with the coupling medium.

The testes were removed at varying times post irradiation, from immediately (within 60 seconds post irradiation) to a few weeks post irradiation, and placed in 10% formalin in ringers fixative for a minimum of 48 hours. A sham irradiation sample was contained within every histological preparation. Standard histological dehydration and paraffin embedding was employed (Thompson, 1966). Six micron sections were prepared to minimize possible confusion concerning the specific stage of spermatogenesis. Adjacent section sets were stained with Hematoxylin and Eosin (H & E) and periodic acid Schiff (PAS). H & E stains nuclear material black and cytoplasm and connective tissue various shades of gray while PAS stains carbohydrates, a main constituent of the acrosome, black and the remaining cellular components various shades of gray. All micrographs are H & E stained unless otherwise indicated.

The stained sections were analyzed first at low power (40X) to detect and classify gross damage to, for example, intra-tubular, extra-tubular, and the connective tissues. The sections then were examined at higher magnifications, (100X to 450X) to detect the specific cell types damaged, alteration of spatial organization and alteration of temporal sequences. This last criterion applied most particularly to the spermiogenic cycle and was evaluated principally from the PAS sections.

RESULTS

Figures 1, 2 and 3 show normal mouse testis in cross-section. The morphology between normals and shams was indistinguishable. Figure 1 shows the seminiferous tubules (T) embedded in a matrix of interstitial cells and encapsulated in a tough, connective tissue shell, the tunica albuginea (TA).

Figure 1. Low power (40X) micrograph of the normal mouse testis. BV-blood vessel, TA-tunica albuginea, T-seminiferous tubule. Bracket represents 100 µm (⊢—⊣).

Figure 2 illustrates the anatomical structure of the mouse testis in greater detail, particularly the densely packed and darkly stained interstitial cells, and the ordered complexity of the tubules. The basement membrane bounding each tubule is visible, as are the lumina which do not have a limiting membrane.

Figure 3 illustrates in greater detail from Figure 2 the structure of two adjacent seminiferous tubules and a variety of different germ cell stages. Here two stem cells are visible, adjacent to, and just below the basement membrane which forms a diagonal in the

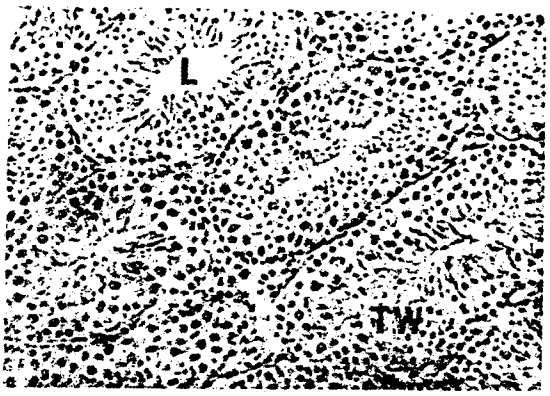

Figure 2. Medium power (100X) micrograph of the normal mouse testis. L-lumen, TW-tubule wall. Bracket represents 50 μm (⊢——⊣).

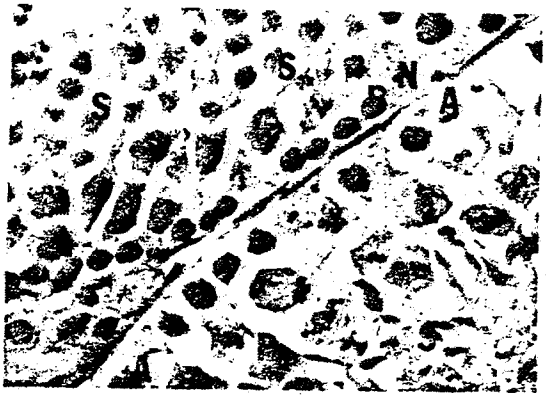

Figure 3. High power (450X) micrograph of the normal mouse testis. A and B-type A and B spermatogonia, P-primary spermatocyte, N-Sertoli cells, S-spermatid. Bracket represents 10 μm (⊢——⊣).

figure. On the opposite side of this membrane the curving line of deeply stained cells are the type B spermatogonia, which are the mitotic offspring of the stem cells via the intermediate stage. The mitotic figures visible in the lower tubular are also type B spermatogonia dividing to form primary spermatocytes. The remaining cells visible in the lower tubule are pachytene primary spermatocytes which have a mottled appearing nucleus, and the thin, tapered slopes of stage 15-16 spermatids (Rugh, 1968) which will be released into the tubule lumen as immature spermatozoa.

Figures 4 through 8 represent sections of testicular tissue exposed to continuous wave ultrasound for 30 sec at an ultrasonic intensity of 25 W/cm^2 and examined as a function of time post irradiation, viz., immediate, 6 hour, 48 hour and 7 day. Under these exposure conditions approximately twelve animals were irradiated and none survived beyond 19 days after irradiation.

The lacework appearance at the top right in Figure 4 is characteristic of the early stages of gross, acoustically induced, damage and the appearance is due to the vacuolization of the tubule wall and sloughing of the germinal epithelium from the basement membrane.

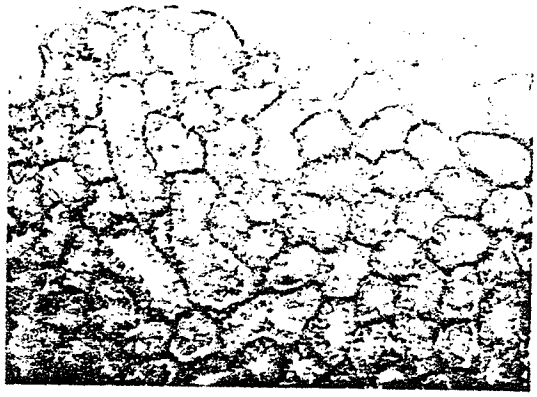

Figure 4. Immediate post irradiation (25 W/cm^2 - 30 sec) mouse testis. 100 μm (⊢——⊣).

These processes are seen in greater detail in Figure 5, which shows a portion of three different tubules, each having large areas devoid of cells, large gaps along the basement membranes and many cells free from an attachment and floating into the lumen.

The breakup of the tubules and interstitial cells is observed in the lower half of Figure 6, which was fixed six hours post irradiation. This damage is characterized by the lack of continuity of tissue between tubules, the loose debris around tubules, and the variety of tubules which appear to

be either fluid filled shells or clogged with cellular debris.

Figure 5. Immediate post irradiation (25 W/cm^2 - 30 sec) mouse testis from the same slide as Figure 4. V-vacuole. 10 μm (⊢—⊣).

Figure 6. Six hour post irradiation (25 W/cm^2 - 30 sec) mouse testis. 100 μm (⊢—⊣).

Figures 7a and 7b show different testis from the same animal at 48 hours post irradiation and demonstrate markedly the wide range of ultrasonically induced damage to testicular tissue which, in some situations, is observed in the same section. Figure 7a exhibits a normal appearance at the left, and a disrupted appearance at the right. The tapered band of tissue at the right edge consists of tubules filled with an amorphous slurry of fluid and cell debris. Figure 7b, on the other hand, shows areas of clear fluid which have apparently replaced destroyed cellular elements. Also, many tubules are completely denuded of the germinal eipthelium along with broken basement membranes, a thickened tunica is visible (top left) and there is a total lack of any interstitial cells (right of center).

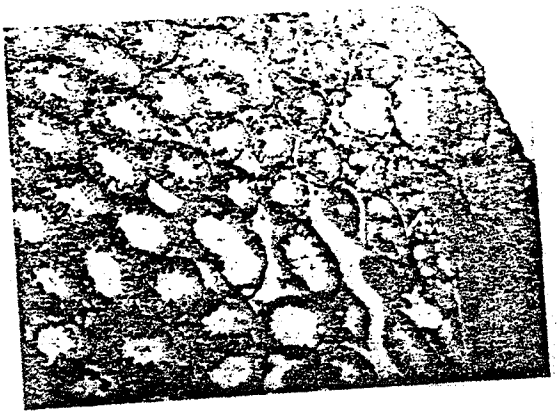

Figure 7a. Fourty-eight hour post irradiation (25 W/cm^2 - 30 sec) mouse testis. Same animal but opposite testis from Figure 7b. 100 μm (⊢—⊣).

Figure 7b. Fourty-eight hour post irradiation (25 W/cm^2 - 30 sec) mouse testis. Same animal but opposite testis from Figure 7a. 100 μm (⊢—⊣).

Figure 8 suggests the appearance of a group of senile, fluid filled tubules in the top half and a group of debris and fluid filled tubules below at 7 days post irradiation. The senile tubules show no vestiges of spermatogenic activity. The fluid suggests ongoing degenerative processes in adjacent volumes of tissue. The thickened

and delaminated tunica is visible adjacent to the fluid-filled tubules.

Figure 8. Seven day post irradiation (25 W/cm^2 - 30 sec) mouse testis. 100 μm (⊢——⊣).

Figures 9 through 21 exhibit, as a function of time post irradiation before sacrifice and fixing, effects on testes exposed for 30 seconds to 10 W/cm^2 continuous wave ultrasound. Here approximately 20 animals have been irradiated and the times post irradiation are immediate, 24 hour, 48 hour, 5 day, 10 day, 19 day, and 43 day.

No damage is suggested in the low power micrograph of Figure 9 where the animal was sacrificied immediately post irradiation. However, at high magnification, fluid accumulations in both intra- and extra-tubular are observed.

Figure 9. Immediate post irradiation (10 W/cm^2 - 30 sec) mouse testis. 100 μm (⊢——⊣).

Figure 10 is a very low power micrograph obtained 24 hrs post irradiation. The acoustic field was incident from the bottom of the section. An examination of the testis on the left side shows an area of destruction extending from the bottom half around and up the right edge. The balance of the left testis and the majority of the right testis, at this magnification, show some interstitial cells to be missing, while the tubules appear normal morphologically.

Figure 10. Very low power (7X) micrograph of a 24 hour post irradiation (10 W/cm^2 - 30 sec) mouse testes. Braket represents 1 mm (⊢——⊣).

Figure 11 is a greater magnification of the apparent boundary between the two disrupted areas shown in Figure 10. The vacuolization of the germinal epithelium is accompanied by debrise and fluid filled lumina. Figures 12 and 13 show in even greater detail the lower part of the testis on the left hand side of Figure 10 detailing the fluid filled appearance of the tubule walls and lumina from the liquifaction of degenerating cells. The PAS stained section (Figure 13) shows the two ovoid, diffuse, pale-stained type B spermatogonia in the top right corner and restingprimary spermatocytes, two of which may be seen just to the right of center at the top of the figure as two mottled, irregular structures. Dark, irregularly stained, late spermatids may also be seen within, and proximal to, the tubule lumen. The morphology of the spermatids

is not normal, but pale and swollen.

Figure 11. Twenty-four hour post irradiation (10 W/cm^2 - 30 sec) mouse testis detailing the apparent boundary in the testis on the left hand side of Figure 10. 100 µm. (⊢—⊣).

Figure 12. Twenty-four hour post irratiation (10 W/cm^2 - 30 sec) mouse testis detailing the debris and fluid filled area in the lower part of the testis on the left hand side of Figure 10. 50 µm (⊢—⊣).

The degree of disruption shown in Figure 14 is representative of testes fixed 48 hours post irradiation wherein the vacuolization of the epithelium (left of center) is suggested by the isolated individual cell clusters and the separation from the basement membrane. The pale diffuse ovoid structures (right of center) are degenerating spermatocytes and intermediate or type B spermatogonia. In the lower right corner both normal and abnormal appearing late spermatids may be seen; the abnormal spermatids appear more globular or rounded.

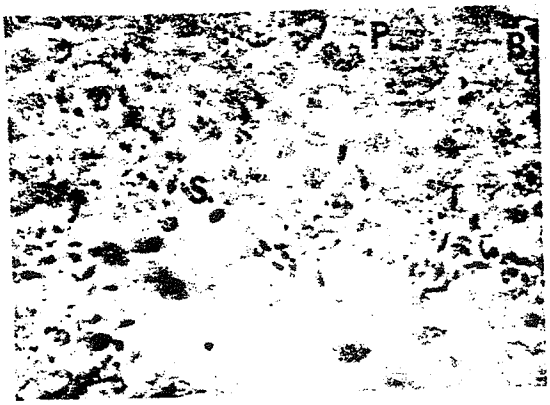

Figure 13. Twenty-four hour post irradiation (10 W/cm^2 - 30 sec) mouse testis detailing the same general area as in Figure 12. PAS stained. S-spermatids, B-type B spermatogonia, P-primary spermatocytes. 10 µm (⊢—⊣).

Figure 14. Fourty-eight hour past irradiation (10 W/cm^2 - 30 sec) mouse testis. V-vacuoles, BM-basement membrane, P-primary spermetocytes, S-spermatids. 10 µm (⊢—⊣).

The loss of cytoplasm from cells of the germinal epithelium, pale disrupted cell nuclei in spermatocytes and

spermatogonia and general breaking up of the tubule walls are all evident in the 5 days post irradiation Figures 15 and 16. Gaps along the basement membrane visible at the top of Figure 15 appear where stem cells have deteriorated. The several pale-stained, amorphous areas throughout the epithelium are indications of abnormal cells. Fluid leakage into the tubule lumen is associated primarily with the spermatids visible at the lumen edge. The

Figure 15. Five day post irradiation (10 W/cm^2 - 30 sec) mouse testis. G-germinal cell gaps, I-intermediate spermatogonia, S-spermatides. 10 μm (⊢——⊣).

PAS stained section in Figure 16 shows spermatid degeneration. The irregularly shaped, dark figures forming an arc about the center of the figure are spermatids which have degenerated and the specific stage of maturation is no longer identifiable.

At 10 days post irradiation the degeneration of the tubules is considerably advanced as shown in Figures 17 and 18. The interstitial damage in general resembles that observed for 6 hours post irradiation damage at the 25 W/cm^2 exposure (see Figure 6). In Figure 17 note the fluid filled and debris filled appearance of the tubules and the thickened tunica. Figure 18 shows the senile appearance of the tubules and the paucity of germ cells. Inordinate amounts of extra-cellular material and many degenerated cells are present. Some mitotic figures are present but no normal spermatids are evident.

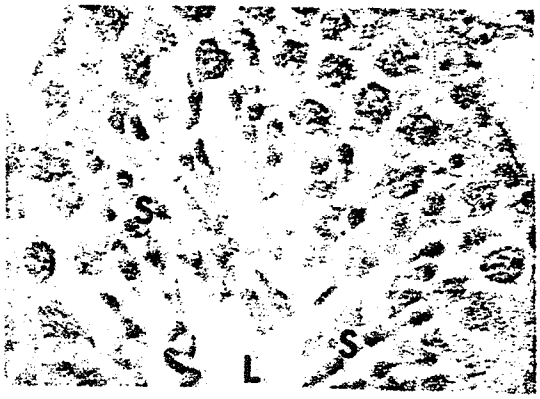

Figure 16. Five day post irradiation (10 W/cm^2 - 30 sec) mouse testis. PAS stained. S-spermatids, L-lumen. 10 μm (⊢——⊣).

Figure 17. Ten day post irradiation (10 W/cm^2 - 30 sec) mouse testis. T-fluid filled tubule. 100 μm (⊢——⊣).

Figure 19 is a 19 day post irradiation PAS section in which no spermatids are visible, an indication that spermatogenesis has ceased.

Figure 20 is a 43 day post irradiation section exhibiting a thin germinal epithelium and the absence of cell types beyond the secondary spermatocytes, the immediate precursor of the spermatid. The PAS section (Figure 21) confirms the absence of spermiogenesis by the absence of acrosomes.

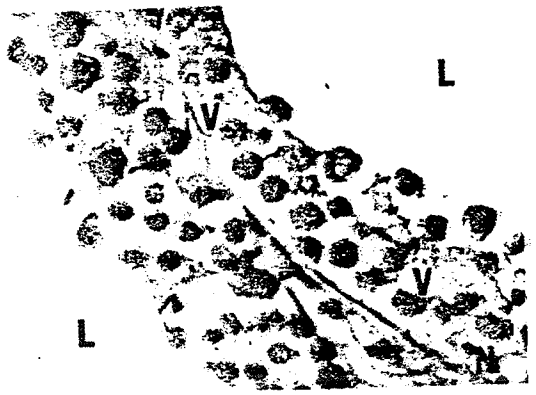

Figure 18. Ten day post irradiation (10 W/cm^2 - 30 sec) mouse testis. V-vacuoles, N-Sertoli cells, P-primary spermatocytes, L-lumina. 10 µm (⊢——⊣).

Figure 20. Fourty-three day post irradiation (10 W/cm^2 - 30 sec) mouse testis. Early spermatid-arrow, S-abnormal spermatids, V-vacuoles, BM-basement membrane. 10 µm (⊢——⊣).

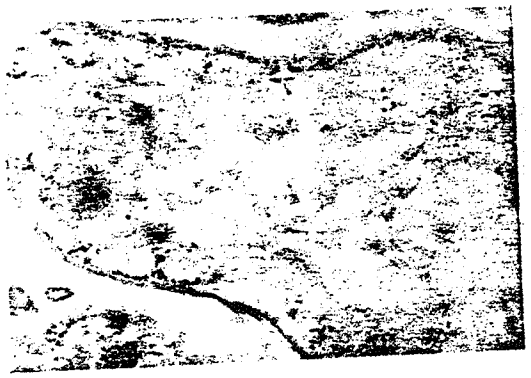

Figure 19. Nineteen day post irradiation (10 W/cm^2 - 30 sec) mouse testis. PAS stained. 10 µm (⊢——⊣).

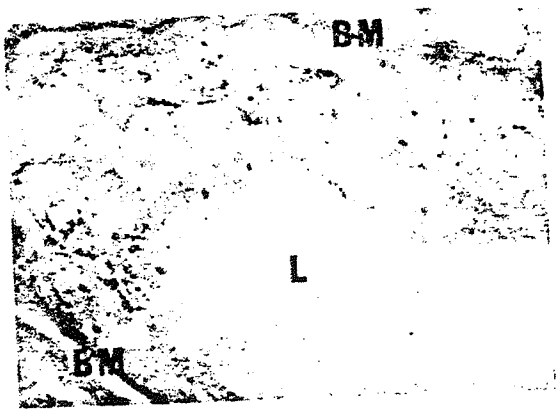

Figure 21. Fourty-three day post irradiation (10 W/cm^2 - 30 sec) mouse testis. PAS stained. BM-basement membrane, L-lumen. 10 µm (⊢——⊣).

DISCUSSION

This preliminary report suggests that ultrasound is capable of markedly disrupting testicular tissue and specifically affecting both spermatocytogenesis and spermiogenesis. Additionally, vacuolization of the extra-tubule elements is observed.

The morphological alteration of testicular tissue is rather different for the two exposure conditions, viz., 25 W/cm^2 for 30 second and 10 W/cm^2 for 30 sec. The principal difference appears to be a delay in the progression of damage sequences, that of the lower intensity requiring several days before any degree of dissolution is observed as compared to the higher intensity exposure wherein damage appears immediately.

There appears to be a suggestion that, given sufficient time post irradiation, the extent of damage at both intensities would be similar. But even so, the type of damage does not appear similar. The higher intensity exposure would completely denude the tubules whereas the lower intensity exposure generally appears to disrupt the spermatogenesis cycle but does not completely denude the tubules.

The spatial distribution of damage across any one preparation is highly variable, and in some cases does not correspond to the free field intensity distribution which is believed to be uniform within 5% across the breadth of the testis for the plane-wave field (Brady et al., 1976). Such a distribution of damage and specifically with regards to adjacent tubules where one appears normal and the other is severely damaged appears to be unique. The closeness of the tubules would provide a basis for suggesting some non-thermal mechanism, such as cavitation-like activity, for producing this highly localized damage.

The damage at the cellular level is varied, depending upon the type of cell examined. In the case of ionizing radiation, the order of sensitivity of germ cells is know (Oakberg, 1956b; Mandl, 1964): the type B spermatogonia are most senstive, followed by intermediate and type A spermatogonia. These are than followed by primary spermatocytes, secondary spermatocytes, spermatids and finally spermatozoa. The Sertoli cells and interstitial cells are very resistant to damage by ionizing radiation (Oakberg, 1956a). This order does not find a parallel in damage caused by ultrasound. Observation of the damage produced at 1 MHz shows spermatocytes to be the earliest influenced cell types in the tissue. Evidence for this is the liquifaction and breaking up of these cells in large numbers as the first signs of damage. The next cell types to show damage are the spermatids, as shown in the 10 day post irradiation (10 W/cm^2 - 30 sec) preparations illustrated by inability of the acrosome to take up the PAS stain. This is further emphasized in the 43 day post irradiation (10 W/cm^2 - 30 sec) preparations where normal appearing early spermatids were identifyable in the H & E preparation, but completely absent, as acrosomal figures, in the PAS stained slide. This observation raises the question of the point of damage to the spermatogonia. Since these cells may appear normal, although depleted, in preparations showing abnormal spermatids, how may damage, other than gross disruption, to be assessed? The method used to date is to follow the time course of degeneration and depopulation, if any, to evaluate actual damage to these cells.

The physical mechanisms responsible for the observed testicular damage are not well understood, but the field of possibilities may be somewhat narrowed. Cavitation is a possibility at the higher intensity level. Although the disruption of the tissue is severe, it is not grossly destroyed as would be expected from transient cavitation. This, however, does not preclude stable cavitation. The possibility of a thermal mechanism is necessary to consider owing to the thermal sensitivity of testicular tissue. At the higher intensity the intrascrotal temperature is measured to be 47-50°C at the end of the exposure. However, at the lower intensity the temperature rise is only 2°C, yielding a final testicular temperature of 39°C. As of now, however, there is no evidence to support any particular mechanism.

ACKNOWLEDGEMENT

The authors acknowledge gratefully the partial support of this study by a grant from the Bureau of Radiological Health, Food and Drug Administration.

REFERENCES

Portions of this work have been extracted from the thesis in preparation by J. K. Brady in partial fulfullment of the requirements for the Ph.D. degree in Electrical Engineering, University of Illinois.

Albright, R. J. and J. H. Harris. "Diagnosis of Urethral Flow Parameters by Ultrasonic Backscatter." IEEE Trans. Biomed. Eng., BME-22, 1-11 (1975).

Brady, J. K., S. A. Goss, R. L. Johnston, W. D. O'Brien, Jr. and F. Dunn. "Ultrasonic Propagation Properties of Mammalian Testes." J. Acoust. Soc. Amer., 60, 1407-1409 (1976).

Dunn, F. and F. J. Fry. "Ultrasonic Field Measurement using the Suspended Ball Radiometer and Thermocouple Probe." In Interaction of Ultrasound and Biological Tissues Workshop Proceedings, eds., J. M. Reid and M. R. Sikov, DHEW Publication (FDA) 73-8008 BRH/DBE 73-1, U. S. Government Printing Office, Washington, D. C., pp. 173-176 (1972).

Hall, L. W. Wrights Veterinary Anesthesia and Analgesia. 7th ed. Bailliere Tindall, London, pp. 224-226 (1971).

Mandl, A. M. "The Radio Sensitivity of Germ Cells." Biological Reviews, 39, 288-371 (1964).

Miskin, M. and J. Bain. "B-mode Ultrasonic Examination of the Testes." J. Clin. Ultrasound, 2, 307-311 (1974).

Monesi, V. "Spermatogenesis and the Spermatozoa." In Germ Cells and and Fertilization, eds., C. A. Austin and R. V. Short, Cambridge University Press, London, pp. 46-84 (1972).

Nalbandov, A. V. Reproductive Physiology of Mammals and Birds. Freeman, San Francisco (1976).

Oakberg, E. F. "A Description of Spermiogenesis in the Mouse and its Use in Analysis of the Cycle of the Seminiferous Epithelium and Germ Cell Renewal." Am. J. Anat., 99, 391-413 (1956a).

Oakberg, E. F. "Duration of Spermatogenesis in the Mouse and Timing of Stages of the Cycle of the Seminiferous Epithelium." Am. J. Anat., 99, 507-516 (1956b).

O'Brien, W. D., Jr. "Ultrasonic Dosimetry." In Ultrasound: Its Application in Medicine and Biology, ed., F. J. Fry, Elsevier Press, The Netherlands, 1977 (in press).

Rugh, R. The Mouse. Burgess Publishing Co., Minneapolis (1968).

Thompson, S. W. Selected Histochemical and Histopathological Methods. Charles C. Thomas, Springfield, Illinois (1966).